

A Convolutional Neural Network Approach to Predicting the Power Output of a Solar Farm

David Ding

Received August 05, 2024

Accepted February 04, 2025

Electronic access February 15, 2025

Solar power is increasingly used as a source of renewable, sustainable energy and a tool in the fight against climate change. However, the high variability of solar power output poses challenges to further implementation into the grid, thus necessitating accurate forecasting of power production. This paper proposes three machine-learning models to forecast the power output of a solar farm using features including temperature, solar radiation, and humidity. Two models forecast future power output at 15-minute and 30-minute prediction horizons, respectively, using the past 24 hours of data, making them useful in currently operating solar farms. Additionally, one model predicts power output in real-time using currently observed features, making it useful for forecasting with a weather forecast available or for hypothetical situations, such as when planning a solar farm. All of the models utilized convolutional neural network (CNN) approaches due to their strength in capturing dependencies in time-series data and time efficiency. Overall, the models had promising performance metrics. The real-time model, 15-minute forecasting model, and 30-minute forecasting model had R^2 scores of 0.971, 0.930, and 0.945, respectively, and had low mean average errors with respect to the average power output. Thus, the models demonstrate the significant promise of CNNs in solar power forecasting.

Introduction

Solar energy has become an effective supplement to traditional energy sources. The increasing use of solar energy significantly reduces greenhouse gas emissions and serves as a sustainable means of generating power. By providing 1.7% of the world's energy, solar power has already become an important renewable energy resource to fulfill the energy needs of society¹. The increased reliance on solar energy makes accurate predictions of solar power generation more important than ever. Solar power generation, however, is variable due to factors like weather conditions and time of day. The grid is not designed for such varying power inputs, as more reserves will be needed to compensate for fluctuations. Thus, accurate short-term prediction of solar power output allows grid operators to better anticipate fluctuations in solar power generation, thereby improving grid stability and ensuring the overall dependability of the system. Accurate prediction thus helps integrate solar energy into the electrical grid and optimize the dispatch of energy from different sources. It can also minimize operational costs and enhance revenue opportunities for renewable energy stakeholders. In fact, one study suggests that if solar penetration increased to 25%, utilizing state-of-the-art forecasting models would reduce net electricity generation costs by 22.9% compared to 12.3% without any forecasting; additionally, curtailment would drop from 34% to 11% with forecasting², demonstrating the importance of solar power forecasting.

Solar photovoltaic (PV) cell technology has proliferated as

a sustainable energy source. There have been at least four generations of solar cell technologies from the first generation of mono or polycrystalline silicon cells to the fourth generation of hybrid materials³. Numerous factors are known to affect solar power output from photovoltaic (PV) solar panels. The two most notable are temperature and solar radiation. For example, PV solar panels typically decrease by 0.5% in efficiency when the temperature increases by 1 degree Celsius⁴. In heatwave conditions, when the temperature increases from 30-50%, the solar panel efficiency drops by 3-9%⁵. The second important factor is solar radiation, or the electromagnetic radiation from the sun including both visible, ultraviolet, and infrared shine, as PV panels convert solar radiation into electrical energy at an efficiency rate of around 7-11%⁶. As a result, weather conditions such as cloud cover or dust, which block visible light, have large effects on power production. Ultraviolet radiation can generate solar power as well, but the amount is much smaller compared to visible sunshine⁷. Additionally, since solar absorb the most energy when sunlight is perpendicular and when irradiance is greater, and these two factors fluctuate with the seasons, seasonal changes can have large effects on solar power output as well; typically summer has the highest power production due to greater solar irradiance and more direct radiation, and this effect is less pronounced at lower latitudes and more pronounced at higher latitudes⁸. Thus, measuring these variables and understanding their impact on solar power production is important for accurate forecasting.

Many approaches have been used to forecast solar energy gen-

eration. These mainly involve statistical and machine-learning approaches. The statistical approach for forecasting relies on statistical models, such as Autoregressive Integrated Moving Average (ARIMA), Autoregressive Moving Average (ARMA), and regression models, which are ideal for forecasting based on time series data. For example, Atique et al. created an ARIMA model to model the power output of a solar panel at a research facility⁹. However, in recent years, much more work has been done to forecast solar power using machine learning predictions. This involves, in most cases, Support Vector Machines (SVM) and neural networks. For example, in 2017, Nageem and Jayabarathi utilized a Multi-Input Support Vector Regression model to predict the power output of a solar panel 8 grid-connected photovoltaic solar panels in Tamil Nadu, a state in India¹⁰. In 2022, a study utilized a Long Short-Term Memory (LSTM) neural network, which is designed for time-series data, to forecast power output using data from a study conducted on a 48 MW plant in Nova Scotia, Canada¹¹. Additionally, in 2024, Saxena et al. utilized a Kth nearest neighbor (KNN) and LSTM hybrid model to forecast power output and achieved an accuracy of 98%¹².

This paper focuses on a machine learning approach to forecasting solar power output, specifically utilizing neural networks. The data utilized for training is from a solar farm in Bou Saada, Algeria, and contains temperature, solar radiation, humidity, and power output measured at 15-minute intervals. Using this data, three models were created, one for predicting power output using real-time data, and two for forecasting power output at 15-minute and 30-minute time horizons, respectively, using the past 24 hours of data. The real-time model is useful in forecasting power production using weather forecasts, or when planning prospective farms. The forecasting models are suitable in currently operating solar farms, as they can work so long as past data is available. Both the real-time and forecasting models demonstrate great potential through their performance metrics.

Methods

Data Overview

The data for the model is taken from a study of a 10,000-kW photovoltaic (PV) solar farm in Bou Saada, Algeria¹³. The data available from the study ranged from January 1, 2019, to January 31, 2019. Some descriptive statistics for that dataset are shown in Table 1 below. The data consists of six features—a time stamp, panel temperature, tilt radiation, direct radiation, total radiation, and humidity, and the label, total power production. Tilt radiation measures the total solar radiation, or electromagnetic waves from the sun, received on the surface of the panels, which are tilted; the amount of tilt radiation depends on both the panel tilt angle as well as the rotation of the Earth, which causes the angle of sunlight to change relative to the panels. Direct

radiation measures the unscattered solar radiation on the normal plane to the incoming sunlight. Total radiation measures the total solar radiation of all of the solar radiation on the normal plane to the incoming sunlight. All three forms of radiation are measured in watts per meter squared (W/m²), the temperature is measured in Celsius (C), and the humidity is measured in percentage (%). The data is collected in 15-minute intervals, resulting in 2975 data points.

In Bou Saada, which has a low latitude, winter months had the highest average photovoltaic energy production and higher volatility than other seasons; spring, summer, and autumn had slightly lower and slightly more stable energy outputs¹⁴. Thus, while a focus on data from only January has limitations in the generalizability of the models for full-time operation, it is a fair representation of the performance of the farm throughout the year.

Data Preprocessing

Before model training, the data was processed to ensure and enhance data quality for optimal training. As mentioned, three models were trained in this study, one for predicting real-time power output based on the features and two for forecasting power output at 15- and 30-minute time horizons in the future using historical data. Different preprocessing steps were involved for the real-time and forecasting models.

For the real-time prediction model, all rows in the data with missing values were removed. Then, the time column was replaced with two new features to make the time variable numerical. Firstly, a “day of the month” feature was added, which tracked the day in January. This was done to allow the model to account for unobserved factors that vary across days but are constant within each day. By controlling for daily fixed effects, the model can focus on variation within days (across other variables of interest) while removing daily-level noise or confounding. Also, a “time of day” feature was added, which started at 1 for 12:15 AM for each day and increased for each time step in the day, ultimately resulting in repeating cycles of 1 to 96. Additionally, all columns were plotted in histograms to ensure that there were no extreme values that could skew the model; none were found. For example, a histogram of the temperature column is shown in Figure 1 below. In Figure 1, there are no significant outliers, and all data points in the histogram are reasonable for temperature, demonstrating that there are no significant issues in this column.

Then, the data was split into training and validation sets with an 80% to 20% ratio. The training set was used to train the model, and the model was tested on the validation set to ensure there was no overfitting. Lastly, the training and validation sets were standardized so that each feature had a mean of 0 and a standard deviation of 1. This was done using the following equation:

Table 1 Descriptive Statistics of the Data

	Mean	Std Dev	Min	25%	50%	75%	Max
Temperature (°C)	13.59	8.92	0.2	7.4	10.5	18.2	47.1
Tilt Radiation (W/m ²)	246.15	390.32	0	0	2.1	402.2	1420.5
Global Radiation (W/m ²)	132.8	210.26	0	0	2	220.2	877
Direct Radiation (W/m ²)	120.44	208.16	0	0	0	159.1	636.7
Humidity (%)	55.69	13.98	15.2	46.6	61.4	66.8	71.9
Power Output (kW)	2021.03	3295.31	-66	-49.5	-44	3371.5	11253

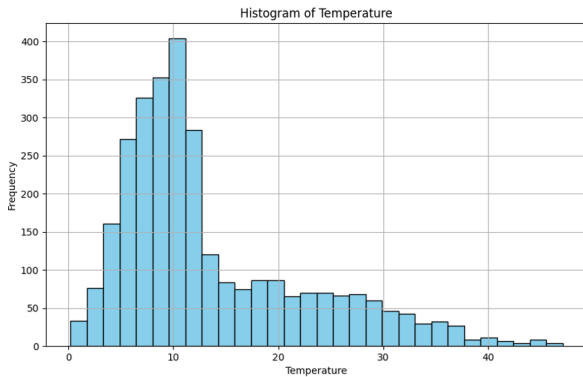


Fig. 1 Histogram of Panel Temperature

$$z = \frac{x - \mu}{\sigma} \tag{1}$$

In the equation above, x represents the current feature variable, μ represents the feature mean, σ represents the feature standard deviation, and z represents the new feature variable. Standardization is a commonly used practice that makes the features more comparable and enhances model robustness.

For the (15-minute and 30-minute) forecasting models, all preprocessing steps described above were also used. However, a few more steps were taken due to the additional complexity of the problem. To allow the two models to predict future power output, a 15-minute, or one-period, and 30-minute, or two-period, lags are used on the total power column. This made the future power output the label for the current features. To allow the models to analyze temporal dependencies, a sliding window approach was used to input current and past features: for each row, the features in that row were combined with the previous 95 rows' features to create the new input for the model. This allowed the model to utilize all of the past 24 hours' data to make the predictions. From there, the data was again split into training and validation sets and the features were standardized according to Equation 1.

Model Development and Training

Traditional fully connected (FC) neural networks consist of an input layer, many hidden layers, and an output layer. Each layer consists of many neurons, and all the neurons in each layer are connected to all the neurons of the next layer through connections. The input layer receives the input features, in this case, the meteorological data. The hidden layers analyze this information, yielding the final output to the output layer. Neurons output information based on the inputs from the previous layer's neurons according to the following equation:

$$O = f \left(b + \sum_{i=1}^N (W_i \cdot I_i) \right) \tag{2}$$

In the equation above, O is the output of the neuron, b is the bias weight, which is unique for every neuron, N is the number of neurons from the previous layer that connect to the current neuron, W_i is the weight of the connection between the current neuron and the i th neuron of the previous layer, and I_i is the output of the i th neuron of the previous layer. f is the activation function for the layer. The most widely used activation function, and the one used in this paper, is the ReLU (rectified linear unit) function, which is shown in Figure 2 below.

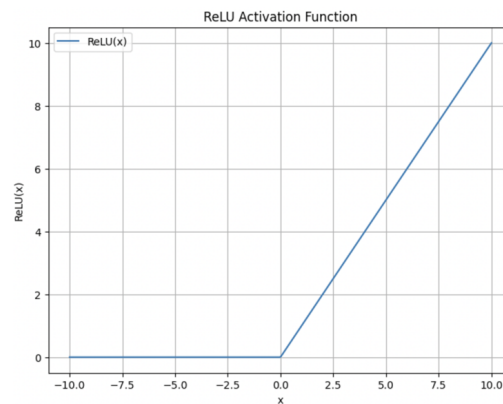


Fig. 2 Graph of the ReLU Activation Function

Convolutional Neural Networks (CNN) are a form of neural network, but unlike conventional fully connected networks, they

utilize a series of convolutional layers before fully connected layers. In the convolutional layers, kernels, or filters, slide over the input data, typically a 2D image, performing convolutions. These filters help identify helpful local patterns and features of the data. Because the filters' weights are applied to the entire layer, they allow for spatial analysis and faster, more efficient training¹⁵.

Despite the prevalence of time series models like LSTMs and GRUs, which are designed to capture sequential dependencies, CNNs have their own advantages for solar power forecasting. This is due to their ability to recognize nonlinear relationships¹⁶ and automatic feature extraction that allows them to perform well in time-series applications¹⁷. In particular, many studies regarding solar power forecasting have utilized hybrid models with CNNs, notably the CNN-LSTM model^{18–20}. However, on their own, CNN models have also shown potential. For example, in one study, a simple CNN, multi-headed CNN, CNN-LSTM hybrid model, ARMA model, and multiple linear regression model were trained to forecast short-term solar power output using a sliding window approach²¹, and results showed that the simple CNN model performed comparably (and often better) than other models, including the CNN-LSTM hybrid. Additionally, CNN models are more time-efficient during training and run an order of magnitude faster than LSTM models²². In experiments, one LSTM model took around 12 hours to train, while one CNN model took around one minute to train; given that thousands of models must be trained in the grid search, a CNN model is more practical. For these reasons, a CNN architecture was utilized for the real-time, 15-minute, and 30-minute models.

Since real-time predictions are not a time series problem, an FC approach was also tested on the real-time model to find the optimal architecture.

The hyperparameters for the models were tuned using a GridSearchCV, or Grid Search Cross-Validation, a tool in the Scikit-learn model selection package. GridSearchCV takes in an input parameter grid with ranges of possible hyperparameter values and performs an exhaustive search by testing every possible hyperparameter combination to find the optimal combination. To assess the performance of each hyperparameter combination, GridSearchCV utilizes k-fold cross-validation. In k-fold cross-validation, the training data is split into k folds. The model is trained on (k-1) folds and validated on the remaining fold. This process is repeated for each fold, and the model's performance is averaged across all k folds, ensuring that the model's performance is robust.

Tables 2 and 3 summarize the grid search input parameter grids for the CNN models and FC model, respectively.

The hyperparameters tuned in the CNN models were batch size, learning rate, kernel size, and number of filters. The number of convolutional layers and pooling layers were also tuned in the grid search to find the best architecture; a pooling layer was

Table 2 CNN Model Grid Search Input Parameter Grid

Parameter	Values
Number of Convolutional Layers	[1, 2, 3]
Number of Pooling Layers	[1, 2]
Number of Filters	[16, 32, 64]
Kernel Size	[3, 5, 7]
Learning Rate	[0.01, 0.001, 0.0001]
Batch Size	[16, 32, 64]

Table 3 FC Model Grid Search Input Parameter Grid

Parameter	Values
Number of FC Layers	[1, 2, 3]
Use Dropout	[0, 1]
Number of Neurons	[32, 64, 128, 256]
Learning Rate	[0.01, 0.001, 0.0001]
Batch Size	[16, 32, 64]

always added after the last convolutional layer, and if the number of pooling layers was 2, the additional pooling layer was added after the first convolutional layer. For the real-time FC model, the hyperparameters tuned were neuron count, learning rate, and batch size. Similarly to the CNN models, the number of fully connected layers and the inclusion of dropout layers—controlled by the binary “Use Dropout” variable (0 for no dropout layers, 1 for a dropout layer after every fully connected layer)—were also included in the grid search to find the optimal architecture.

In the CNN model, following the convolutional and pooling layers, a flattening layer, a dense layer with 64 neurons, and a final output layer were also added. In the FC model, after the fully connected layers, a final output layer was added.

Additionally, for both the real-time FC and CNN models, only current features were inputted (i.e. no sliding window) for simplicity and because the current power output is primarily dependent on immediate features. As such, the kernel sizes of 3, 5, and 7 in the grid search for the 15-minute and 30-minute CNN models are too large; kernel sizes of 1, 2, and 3 are utilized for the grid search on the real-time CNN model.

For all models, an early stopping program, which stopped training when the validation loss stopped improving for 15 epochs and restored the past weights that produced the lowest loss, was utilized to prevent overfitting.

Results

The three metrics used to measure the performance of the models were mean absolute error (MAE), mean squared error (MSE), and the coefficient of determination (R^2). MAE measures the average of the absolute error of the model, MSE measures the average of the squares of the model error, increasing the impact

of large errors, and R^2 measures the percentage of the variance in the total power output that is explained by the model. The formulas for each metric are listed below.

$$MAE = \frac{1}{n} \sum_{i=1}^n |\hat{y}_i - y_i| \quad (3)$$

$$MSE = \frac{1}{n} \sum_{i=1}^n (\hat{y}_i - y_i)^2 \quad (4)$$

$$R^2 = 1 - \frac{\sum_{i=1}^n (y_i - \hat{y}_i)^2}{\sum_{i=1}^n (y_i - \bar{y})^2} \quad (5)$$

In the equations above, n represents the size of the observed set, y_i represents the observed value, \hat{y}_i represents the predicted value, and \bar{y} represents the mean of the observed set.

For the real-time model, the CNN architecture (batch size = 32, filters = 64, kernel size = 2, learning rate = 0.001, Number of Convolutional Layers = 2, Number of Pooling Layers = 2) produced better results compared to the FC approach, with an MAE, MSE, and R^2 score of 209, 304134, and 0.971 respectively. Compared to the average power output of around 2021 kW, the MAE is quite low. The FC architecture was only slightly worse, with an MAE, MSE, and R^2 score of 214, 320681, and 0.969, respectively.

For the 15-minute forecasting model, the grid search yielded the following optimal parameters: batch size = 64, filters = 32, kernel size = 7, learning rate = 0.001, Number of Convolutional Layers = 3, Number of Pooling Layers = 1. This architecture, trained with a learning rate of 0.001 and batch size of 64, yielded an MAE, MSE, and R^2 of 423.5, 778490, and 0.930, respectively.

The grid search for the 30-minute model yielded the exact same parameters as the 15-minute model; this yielded an MAE, MSE, and R^2 score of 380, 626822, and 0.945, respectively²³.

Discussion

Unsurprisingly, the real-time model performed the best, and the forecasting models performed slightly worse. This is because the power production in real-time is essentially some function of the features, which is easy for the neural network to identify. However, forecasting future power output with the current and past features is much harder, as the features do not always follow a predictable pattern. For example, there could be sudden cloud cover or rain that is impossible to predict with the past features, decreasing the accuracy of the model. Nevertheless, the forecasting models were still very accurate.

Along with the performance metrics, the model predictions are also plotted with the observed values for all three models, as shown in Figures 3a-c below. In the plots, the actual power output is plotted in blue, and the model's prediction is plotted in orange; the time axis represents the indices of the observations

(i.e. the 2000th time step corresponds with the 2000th observation). It is important to note there are 96 observations per day. Each day in the plot can be seen starting at 0 kW power output before spiking to around 10000 kW, and then dropping back to 0 kW. The plot shows that the real-time prediction model is very accurate and well-fit to the data, as the orange lines match the blue lines almost perfectly in Figure 3a.

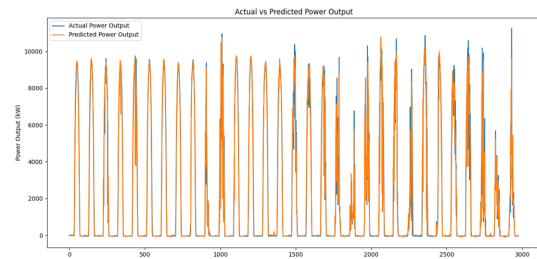


Figure 3a. Graph of Real-time Model Prediction and Observed Power Output

The forecasting models are very accurate on average days, such as the first eight days shown in Figures 3b and 3c below, where the daily power production follows a predictable pattern, and the model's predictions mirror the observed values well. Presumably, these days are all very similar, with clear skies and no weather conditions that affect the power production drastically. This means that the forecasting models can identify and predict the periodic nature of the power production, and thus fit the data well. However, on the days where power production is higher or lower than usual, such as on the tenth and nineteenth days (tenth and nineteenth peaks in the graph), the models are less accurate. On these more abnormal days, the models often underestimate the power production, as shown by the orange peaks being below the blue peaks in Figures 3b and 3c. In short, the models struggle with adaptability to diverse weather conditions. This is likely because the model is biased toward the average days, which dominate the data. This could potentially be solved with feature engineering or inputting more training data to allow the model to train for more conditions.

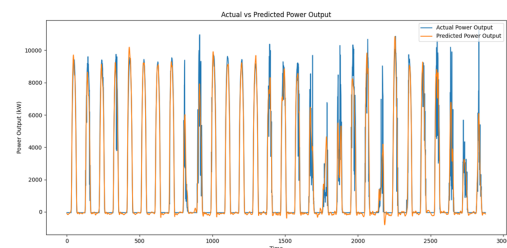


Figure 3b. Graph of 15-minute Forecast Model Prediction and Observed Power Output

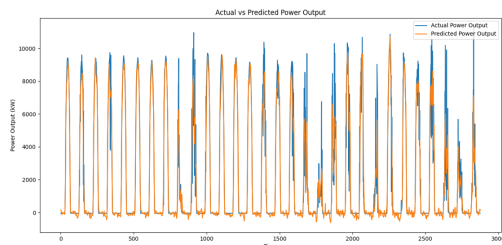


Figure 3c. Graph of 30-minute Forecast Model Prediction and Observed Power Output

Conclusion

This study proposes a real-time prediction model as well as two forecasting models, one at a prediction horizon of 15 minutes and the other at 30 minutes. The real-time model is suited for cases when weather forecasts are available or for investigation of power output in hypothetical scenarios, such as when planning for a prospective solar farm. The forecasting models are more versatile and predict so long as past measurements are available, making them useful for forecasting in currently operating solar farms. In these models, CNNs were utilized due to their strength in time-series forecasting and automatic feature extraction. For the forecasting models, a sliding window approach was utilized to allow the model to forecast based on the past 24 hours' data (96 observations). In each model, different architectures were tested to find the optimal architecture.

Overall, the models trained demonstrated significant potential according to their performance metrics, MAE, MSE, and R^2 , and based on the plots of the predictions and observed values. The models had low MAE and MSE relative to the average power output. The real-time model had an R^2 value of 0.971, the 15-minute forecasting model had an R^2 value of 0.930, and the 30-minute forecasting model had an R^2 value of 0.945. Additionally, when plotted, all models' predictions matched the observed values closely.

Overall, this study has presented both real-time and forecasting models of solar power output, both with unique applications. They have demonstrated significant potential and efficacy based on their performance metrics and plots of the predictions and observations. Although the models in this study perform somewhat below state-of-the-art benchmarks²⁴, it is important to note that they were trained on significantly smaller datasets and with limited computational resources. Additionally, since the dataset used in this study is limited to one month and one location only and there are high variations in solar power generation across locations and seasons, the generalizability of the models to other scenarios is limited. Despite these constraints, the results demonstrate that CNNs can be effective for solar power forecasting. Thus, this study has significant potential impact in advancing the field. In the future, more research can be done to obtain

more data to allow the models to account for seasonal changes in power output as well as variation across locations, feature engineering to address inaccuracies on abnormal days, and more complex models to capture dependencies more accurately.

Acknowledgments

The author expresses gratitude to Dr. Guillermo Goldshtein from Georgia Institute of Technology and Ms. Joanna Gilberti for their guidance and insightful discussions in the writing of this paper.

References

- 1 O. Aldosari, S. Batiyah, M. Elbashir, W. Alhosaini and K. Nallaiyagounder, *Performance evaluation of multiple machine learning models in predicting power generation for a Grid-Connected 300 MW solar farm*.
- 2 C. Martínez-Anido, A. Florita and B. Hodge, *The impact of improved solar forecasts on bulk power system operations in ISO-NE*.
- 3 N. Kant and P. Singh, *Review of next generation photovoltaic solar cell technology and comparative materialistic development*.
- 4 C. Martínez-Anido, A. Florita and B. Hodge, *The impact of improved solar forecasts on bulk power system operations in ISO-NE*.
- 5 A. Patt, S. Pfenninger and J. Lilliestam, *Vulnerability of solar energy infrastructure and output to climate change*.
- 6 S. Kurpaska, J. Knaga, H. Latała, J. Sikora and W. Tomczyk, *Efficiency of solar radiation conversion in photovoltaic panels*.
- 7 B. Parida, S. Iniyana and R. Goic, *A Review of Solar Photovoltaic Technologies*.
- 8 O. Bamisile, C. Acen, D. Cai, Q. Huang and I. Staffell, *The environmental factors affecting solar photovoltaic output*, <https://doi.org/10.1016/j.rser.2024.115073>.
- 9 S. Atique, S. Noureen, V. Roy, V. Subburaj, S. Bayne and J. Macfie, *Forecasting of total daily solar energy generation using ARIMA: A case study*, <https://doi.org/10.1109/ccwc.2019.8666481>.
- 10 R. Nageem and R. Jayabarathi, *Predicting the power output of a Grid-Connected solar panel using Multi-Input Support vector regression*.
- 11 M. Elsaraiti and A. Merabet, *Solar power forecasting using deep learning techniques*.
- 12 N. Saxena, R. Kumar, Y. Rao, D. Mondloe, N. Dhapekar, A. Sharma and A. Yadav, *Hybrid KNN-SVM Machine Learning Approach for Solar Power Forecasting*.
- 13 L. Boucetta, Y. Amrane, A. Chouder, S. Arezki and S. Kichou, *Enhanced forecasting accuracy of a Grid-Connected photovoltaic power plant: a novel approach using hybrid variational mode decomposition and a CNN-LSTM model*.
- 14 L. Boucetta, Y. Amrane, A. Chouder, S. Arezki and S. Kichou, *Enhanced forecasting accuracy of a Grid-Connected photovoltaic power plant: a novel approach using hybrid variational mode decomposition and a CNN-LSTM model*.

-
- 15 L. Alzubaidi, J. Zhang, A. Humaidi, A. Al-Dujaili, Y. Duan, O. Al-Shamma, J. Santamaria, M. Fadhel, M. Al-Amidie and L. Farhan, *Review of deep learning: concepts, CNN architectures, challenges, applications, future directions*.
 - 16 L. Boucetta, Y. Amrane, A. Chouder, S. Arezki and S. Kichou, *Enhanced forecasting accuracy of a Grid-Connected photovoltaic power plant: a novel approach using hybrid variational mode decomposition and a CNN-LSTM model*.
 - 17 L. Sadouk, *CNN Approaches for Time Series Classification*, <https://doi.org/10.5772/intechopen.81170>.
 - 18 C. Obiora and A. Ali, *Hourly photovoltaic power forecasting using CNN-LSTM hybrid model*, <https://ieeexplore.ieee.org/document/9615335>.
 - 19 A. Agga, A. Abbou, M. Labbadi, Y. Houm and I. Ali, *CNN-LSTM: An efficient hybrid deep learning architecture for predicting short-term photovoltaic power production*, <https://doi.org/10.1016/j.epsr.2022.107908>.
 - 20 M. Abumohsen, A. Owda, M. Owda and A. Abumihsan, *Hybrid Machine learning model combining of CNN-LSTM-RF for time series forecasting of SPG. e-Prime*, <https://doi.org/10.1016/j.prime.2024.100636>.
 - 21 V. Suresh, P. Janik, J. Rezmer and Z. Leonowicz, *Forecasting Solar PV Output Using Convolutional Neural Networks with a Sliding Window Algorithm*, <https://doi.org/10.3390/en13030723>.
 - 22 H. Weytjens and J. Weerd, *Process Outcome Prediction: CNN vs. LSTM (with Attention)*, <https://doi.org/10.1007/978-3-030-66498-5>.
 - 23 *Baseline ARIMAX models for current, 15-minute, and 30-minute forecasts were trained on the data. ARIMAX models were chosen to incorporate the exogenous variables into the ARIMA forecasts. The real-time ARIMAX performed well, achieving an MAE of 629, while the 15-minute and 30-minute models performed extremely poorly, achieving MAEs of 1564 and 1455, respectively. In all cases, the CNN models performed significantly better. Additionally, FC models were trained on the 15-minute and 30-minute time horizons as well, and they performed significantly worse than the CNN models; no FC model achieved an R-squared over 0.9 on any time horizon.*
 - 24 L. Boucetta, Y. Amrane, A. Chouder, S. Arezki and S. Kichou, *Enhanced forecasting accuracy of a Grid-Connected photovoltaic power plant: a novel approach using hybrid variational mode decomposition and a CNN-LSTM model*.